Research article

Enhancing the filtration performance of common substrates used in the Covid-19 respiratory protection equipment with nanofiber coatings

Mobina Khezrian [a], Adel Jafari [b,c], Majid Habibi Mohraz [b,c,*]

[a] Student Research Committee, Hamadan University of Medical Sciences, Hamadan, Iran
[b] Occupational Health and Safety Research Center, Institute of Health Sciences and Technologies, Avicenna Health Research Institute, Hamadan University of Medical Sciences, Hamadan, Iran
[c] Center of Excellence for Occupational Health Engineering, School of Public Health, Hamadan University of Medical Sciences, Hamadan, Iran

ARTICLE INFO

ABSTRACT

With the emergence of the COVID-19 pandemic, there has been a significant increase in the demand for facemasks as an effective means of protection. As a result, a variety of materials, including woven and nonwoven fabrics, have been utilized as filtration mediums in respiratory protection equipment (RPEs). However, many of these RPEs, despite their widespread use, do not provide adequate protection against aerosols and bioaerosols. Recent studies have demonstrated that nanofiber coatings possess properties that can enhance the protective capabilities of RPEs.

The purpose of this study was to investigate the effects of applying nanofiber coatings on the filtration properties of common substrates used in RPEs. Specifically, polyacrylonitrile (PAN) and PAN modified with CuBTC nanofibers (PAN/CuBTC) were coated onto seven common types of substrates used in RPEs: two types of melt-blown fabric with grammages of 15 and 25 g/m^2, two types of spunbond fabric with grammages of 25 and 30 g/m^2, SSMMS fabric with a grammage of 25 g/m^2, activated carbon fabric, and Tetron fabric. The initial filtration efficiency, pressure drop, and quality factor of the prepared media were then measured.

The results clearly indicated that the application of PAN and PAN/CuBTC nanofiber coatings significantly enhances the filtration efficiency of all examined substrate layers, achieving efficiencies exceeding 90 % and 95 % at the most penetrating particle size (MPPS, 300 nm), respectively.

The assessment of the quality factor revealed that the highest quality factor values before and after coating with PAN and PAN/CuBTC nanofibers corresponded to the SSMMS substrates, with values of 0.023, 0.072, and 0.094 Pa^{-1}, while the lowest quality factor values were associated with Tetron, which had values of 0.002, 0.016, and 0.021 Pa^{-1}, respectively.The comparison of various substrates revealed that the SSMMS fabric exhibited the highest quality factor after coverage with nanofibers, while the Tetron fabric demonstrated the lowest quality factor.

Based on the quality criteria, the SSMMS fabric was the best substrate for nanofiber coatings, followed by melt-blown, spun bond, and activated carbon fabrics, whereas the Tetron fabric was not recommended for this application due to a high respiratory pressure drop.

* Corresponding author. Center of Excellence for Occupational Health Engineering, Occupational Health and Safety Research Center, School of Public Health, Hamadan University of Medical Sciences, P.O.BOX: 6517838736, Hamadan, Iran.
E-mail address: m.habibi@umsha.ac.ir (M.H. Mohraz).

1. Introduction

The COVID-19 pandemic, along with the increasing burden of air pollution, has prompted the scientific community to develop new efficient materials for respiratory protection [1].Personal protective equipment (PPE) is critical for protection against air pollutants and bioaerosols, such as the coronavirus. The filtration efficiency and respiratory pressure drop are the most significant parameters for evaluating the quality of respiratory protection equipment (RPEs); RPEs that exhibit high filtration efficiency and minimal respiratory pressure drop are more practical and comfortable for users [2,3].

During the COVID-19 outbreak, the rising demand for respiratory protective equipment led to the utilization of various woven and nonwoven fabrics, including melt blown, spunbond, activated carbon, and Tetron, either individually or in combination, to manufacture RPEs [4–6].

However, these substrates alone often do not provide the required filtration efficiency. Consequently, multiple layers are typically incorporated into the structure of RPEs to enhance efficiency. Unfortunately, this multilayered design can increase the respiratory pressure drop, leading to discomfort for users [7,8].

Recent studies have indicated that electrospun nanofiber coatings present a suitable alternative to commonly used substrates due to their unique properties, such as small fiber diameters, adjustable pore structures, high surface-area-to-volume ratios, strong interconnectivity, minimal polymer consumption, ease of mass production, and high filtration efficiency with reduced thickness and fewer layers compared to traditional substrates [9–11].

Additionally, research has shown that functionalizing nanofibers with materials like metal-organic frameworks, carbon nanotubes, and other nanoparticles can further enhance the performance of these substrates and impart new properties [12–15].

For instance, Zhang et al. investigated the combination of polyacrylonitrile (PAN) nanofibers with zeoliticimidazolate frameworks (ZIF) for particle filtration, concluding that the ultrafine particle removal efficiency of the designed filter was approximately 99.1 % [16].

Despite the advantageous properties of nanofibers in filtration applications, their very low thickness leads to weak structural integrity, necessitating their use as coatings on supporting microfiber substrates [17,18].

In fact, the conventional substrates utilized in RPEs often suffer from low filtration efficiency and the nanofiber coatings lack adequate structural resilience. It appears that the integration of these two media could result in the development of high-performance RPEs. The primary objective of the present study was to investigate suitable supporting microfiber substrates for nanofiber coatings among the commercially available options used in RPEs as well as to assess the feasibility and degree of enhancement in the filtration properties of existing substrates through the application of nanofibrous coatings.

In the present study two types of Polyacrylonitrile (PAN) and Polyacrylonitrilefunctionalized with MOF-199 (PAN/CuBTC) nanofibers were coated on the 7 types of commercially available fabrics(two types of meltblown fabric with 15 and 25 g/m2grammage, two types of spunbond fabric with 25 and 30 g/m2 grammage, SSMMS fabric with 25 g/m2 grammage, Carbon active fabric, and Tetron fabric) which were used in the structure of RPEs during the Corona pandemic. Finally, the filtration efficiency, respiratory pressure drop and the quality factor of the substrates were evaluated before and after coating with PAN and PAN/CuBTCnanofibers.

2. Experimental

2.1. Materials

Analytical-grade polyacrylonitrile (PAN, Mw = 150,000, g/mol) was provided by Poly Acryl Isfahan Co. (Iran).Benzenetricarboxylic acid, copper acetate, ethanol and N, N-Dimethylformamide (DMF), NaClwas purchased from Merck Co, Germany. All chemicals were of analytical grade, and utilized without further purification.

2.2. Synthesis of MOF-199 (HKUST-1)

Synthesis of MOF-199 was executed in accordance with established protocols detailed by Hanh et al. [19]. Initially, a precise stoichiometric quantity consisting of 4.38 g of copper(II) nitrate trihydrate ($Cu(NO_3)_2 \cdot 3H_2O$) and 0.236 g of benzenetricarboxylic acid (denoted as H_3BTC) was diligently dissolved in a solvent mixture comprising 4 ml of ethanol, 3 ml of DMF, and 2 ml of deionized water. This resultant solution was subjected to isothermal heating for a duration of 24 h at a controlled temperature of 85 °C, leading to the formation of light blue crystals indicative of the desired metal-organic framework. Following synthesis, the resultant solid product was isolated through decantation of the mother liquor and subjected to multiple washes with DMF (each wash comprising 8 ml, performed three times) post-cooling to ambient temperature. Subsequently, an ethanol exchange step was performed using the same volume and frequency. The final product, characterized as purple crystals of MOF-199 with the molecular formula $Cu_2(C_9H_3O_6)_{4/3}$, underwent a rigorous vacuum drying process at 170 °C for 6 h, yielding a net mass of 0.298 g of the synthesized framework.

2.3. Preparation of electrospunnanofibers

Two types of polymeric solutions, PAN and PAN/CuBTC, were prepared according to the following steps. PAN solution composed of 16 wt% was generated by dissolving 1.510 g of PAN in 10 mL of DMF, which was thoroughly stirred for a period of 24 h at room temperature (25 ± 3 °C). In parallel, a PAN/CuBTC solution, optimized to a weight ratio of 7/3, was synthesized by incorporating

0.456 g of CuBTC powder into the pre-prepared PAN solution, followed by an additional stirring period of 24 h to ensure the formation of homogeneous electrospinning solutions. These polymeric solutions were subsequently loaded into a 23-gauge syringe affixed to a metal nozzle and applied onto designated substrates utilizing the ES2000 electrospinning apparatus from Fanavaran Nano Meghyas Co. in Iran, following specified conditions as detailed in Table 1.

2.4. Characterization

The morphological characteristics of substrates and prepared nanofibers was analyzed by Hitachi S4800 (Tokyo, Japan) scanning electron microscopy (SEM). SEM images were analyzed with ImageJ (NIH, USA) image analysis software to estimate the average diameter of the fibers. Fiber diameters were evaluated at 50 different points for each sample.

The base weights (mass of the nanofibers per unit area) of substrates and prepared nanofibers were measured using microbalance (MXA-5, Radwag, Poland). Fourier transform-infrared (FT-IR) spectra were recorded in the range $4000-400$ cm^{-1} by a lambda 950 spectrophotometer using KBr pellets.

2.5. Filtration performance evaluation

Followingcoating nanofibers on the substrates, the samples were cut into suitable dimensions and evaluated by the filtration test rig. Fig. 1 shows the schematic of filtration test rig.

As shown in Fig. 1, the filtration test rig was consisted of four main parts, including the test aerosol generator (collision nebulizer and diffusion dryer) (4920, HCT Co., Ltd., Korea).

The filter sample holding part, which was consisted of a tubular holder with a diameter of 9 cm and two probes before and after the holder to determine concentration of particles and the pressure drop of the samplesunder a face velocity of 10 cm/s and the third part was included an optical particle counter (Model 1.1.09, Grimm Technologies Inc., Douglasville, GA, USA) to determine the count concentration of particles in the size range of 280 nm to 3 μm in diameter and the fourth part was air flow adjustment which was included air pump andflow measuring rotameter.

A filtration media that can create a higher filtration efficiency by applying a minimal respiratory pressure drop is a desirable media. After measuring the filtration efficiency and pressure drop (Kimo, CP 110, France) of each sample, the quality factor (QF), often known as a figure of merit was used to compare the filtration performance of the studied media.

The filtration efficiency (E), particle penetration (P) and quality factor (QF)are formulated as follows [20]:

$$\text{Filtration Efficiency } (\%) = (1 - P) \times 100$$

$$\text{Penetration } (\%) = C_{in}/C_{out} \times 100$$

$$QF = \frac{-\ln(1 - E)}{\Delta P}$$

Here, ΔP and E are the pressure drop and filtration efficiency of the substrates. All experiments were performed at a temperature of 20 °C–25 °C and a relative humidity of 25 %–30 %.

3. Results and discussion

Fig. 2 presents the FTIR spectrum of the synthesized Cu-BTC, exhibiting distinctive peaks within the range of 1700-450 cm^{-1}. Notably, the peak at 486 cm^{-1} is attributed to the copper-oxygen bond, while the peaks at 732 cm^{-1} and 758 cm^{-1} indicate copper substitution in benzene groups, serving as key characteristics of the synthesized metal-organic framework. The peaks at 1374 cm^{-1} and 1447 cm^{-1} correspond to the symmetric stretching vibrations of COO from carboxylate groups in H3BTC. Additionally, the peak at 1113 cm^{-1} relates to the C-O-Cu stretching vibration, and the peak at 1617 cm^{-1} is ascribed to H-O-H vibrations, with the peak at 3423 cm^{-1} associated with hydroxyl groups. These results align with previously reported FTIR spectra for Cu-BTC, thereby confirming the successful synthesis of Cu-BTC [21,22].

Table 1
Electrospinning process parameters for coating nanofibers on the studied substrates.

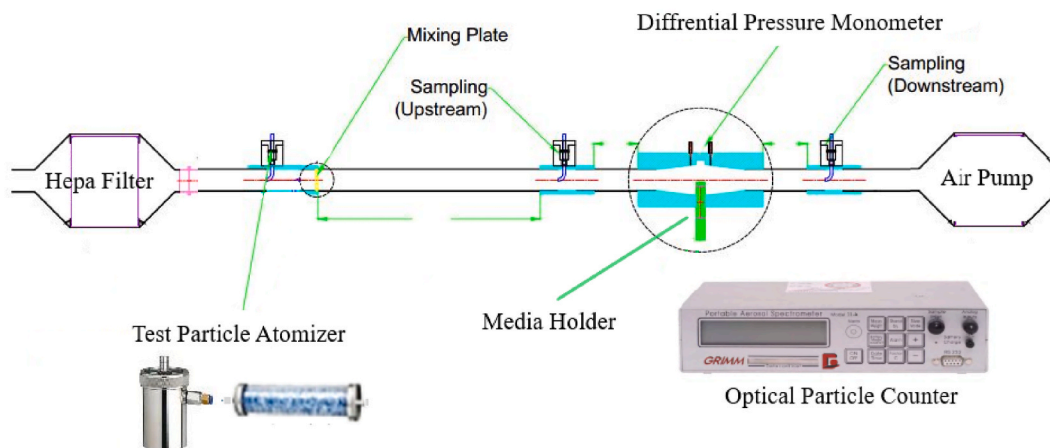| Parameter	Value
Electrospinning deposition time	20 min
Injection rate	0.75 ml/hour
Electrospinning voltage	20 kV
Needle-collector distance	10 cm
Air temperature	$(21\,°C - 24°C)$
Air humidity	25 %_35 %
Needle Diameter	1.2 mm
Rotating drum speed	700 RPM

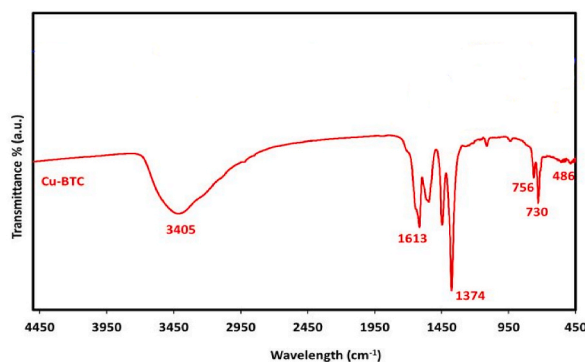**Fig. 1.** The schematic of filtration test rig.

Fig. 2. FTIR spectra of synthesized CuBTC.

SEM images and structural properties of the examined substrates, along with PAN and PAN/CuBTC nanofiber coatings, are presented in Table 2.

The results of Table 2 indicated that the Spunbond substrates, including SB 25, SB 30, and SSMMS, had mean fiber diameters of 15343, 14495, and 14121 nm, respectively, making them the largest in fiber diameter. The Activated Carbon and Tetron substrates, with mean fiber diameters of 12023 and 11320 nm, had medium fiber diameters. Meltblown substrates, including MB 15 and MB 25, had mean fiber diameters of 3366 and 2740 nm, indicating smaller fiber diameters. The lowest fiber diameters were associated with PAN and PAN/CuBTC substrates, which had mean fiber diameters of 332 and 227 nm, respectively. Khodeh, in a review study titled "Nanofibers for High Efficiency Filtration," concluded that the fiber diameters of common substrates, melt-blown substrates, and nanofibers ranged from 10 to 40 μm, 1–5 μm, and 50–500 nm, respectively, which aligns with the findings of the present study [23].

The diameter of the fibers significantly influences the filtration efficiency of filter fabrics, as it is directly related to the various filtration mechanisms of the filters. Fibers with a smaller diameter have a higher efficiency for capturing particles through the mechanisms of direct interception and diffusion, while fibers with a larger diameter contribute more to the inertial based mechanisms such as inertial impaction [24,25]. However, reducing the diameter of the fibers also decreases their mechanical strength; thus, it is necessary to use reinforcing substrates with larger fiber diameters to maintain their physical structure. The fiber diameter not only affects filtration efficiency but also impacts the pressure drop across the filters. Some studies have shown that in nanofibers, due to the presence of slip flow at the filter surfaces, there is a lower pressure drop against airflow compared to the predicted values [26,27].
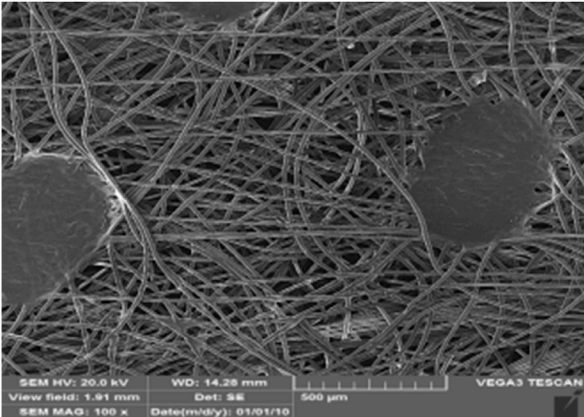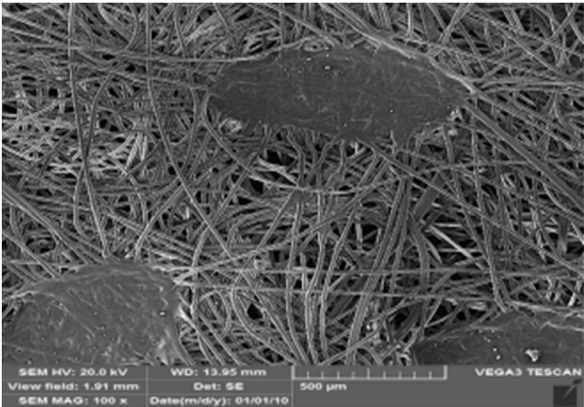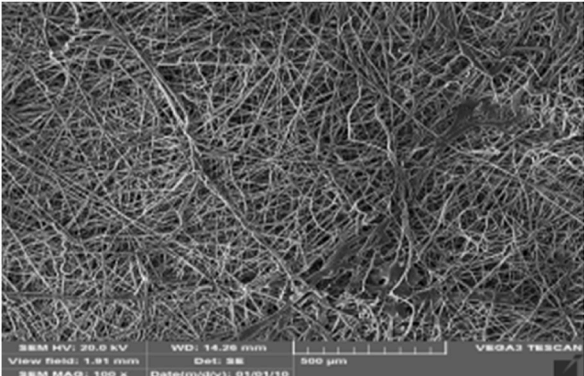
Additionally, the results indicated that the Tetron substrate, with a base weight of 96.4 g/m^2, had the highest base weight, followed by activated carbon, SB30, SSMMS, SB25, and MB15. The lowest base weights were associated with PAN/CuBTC and PAN substrates, with values of 0.121 and 0.139 g/m^2, respectively. Considering that a low base weight indicates less material consumption in substrates, and that reducing base weight also decreases the pressure drop across the substrates, those that can achieve high filtration efficiency with lower pressure drops at reduced base weights are ideal for filtration applications [28,29].

3.1. Substrate filtration performance

Mean filtration efficiency (MFE-300 nm) for the most penetrating particle size (MPPS, 300 nm), pressure drop (DP), and quality
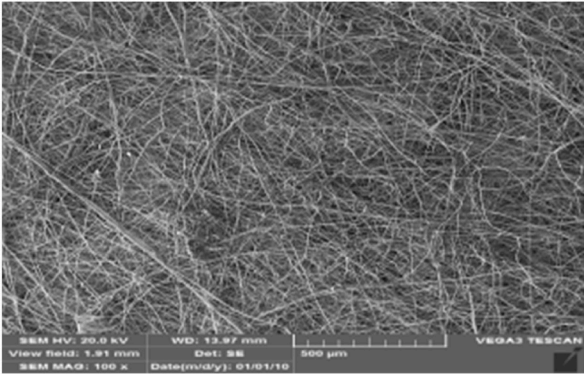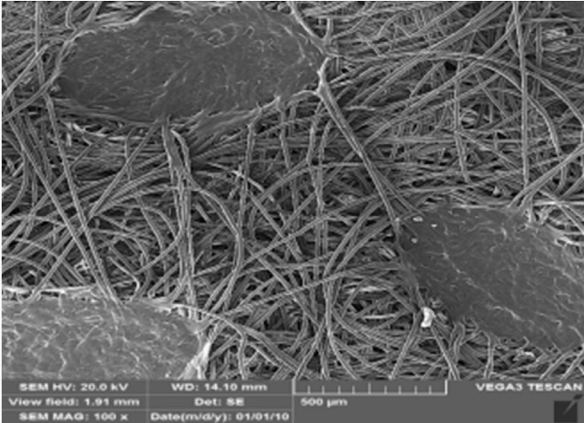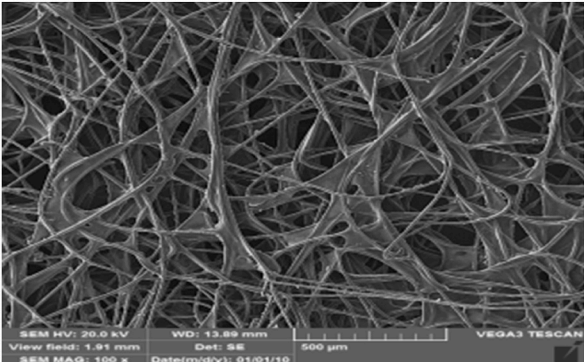
Table 2
SEM images and structural propertiesof studied substrates and PAN, PAN/CuBTC nanofibers.

Sample code	Substrate	BaseWeight (g/m2)	Average fiber diameter (nm)	SEMmicrograph
SB25	Spunbond	24.843	15343 ± 845	
SB30	Spunbond	30.365	14495 ± 743	
MB15	Melt Blown	14.875	3366 ± 482	

Table 2 (*continued*)

Sample code	Substrate	BaseWeight (g/m2)	Average fiber diameter (nm)	SEMmicrograph
MB25	Melt Blown	25.145	2740 ± 423	
S	SSMMS	30.121	14121 ± 875	
C	Activated Carbon	39.121	12023 ± 941	

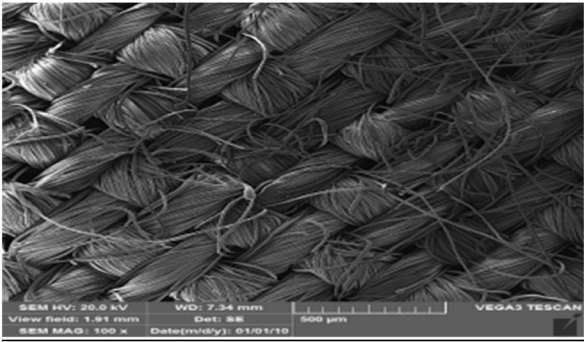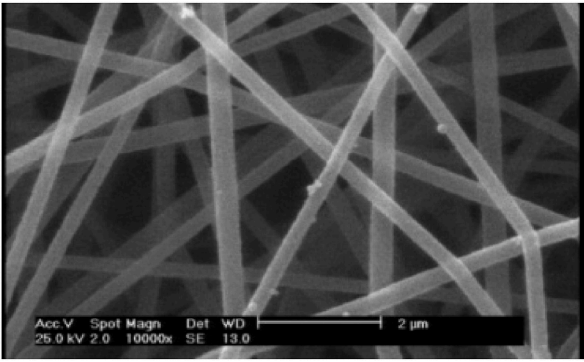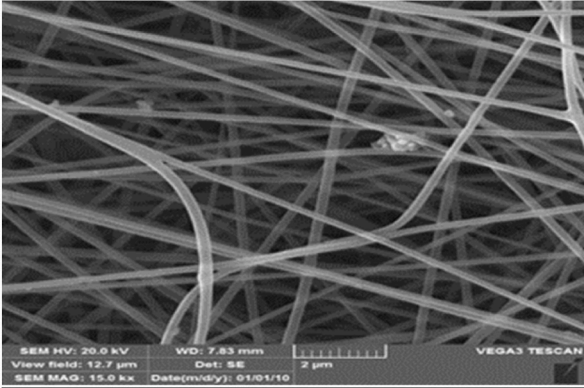**Table 2** (*continued*)

Sample code	Substrate	BaseWeight (g/m2)	Average fiber diameter (nm)	SEMmicrograph
TF	Tetron	96.402	11320 ± 426	
PAN	Polyacrylonitril nanofibers	0.139	332 ± 41	
PAN-CUBTC	PAN-CuBTC nanofibers	0.125	227 ± 16	

factor (QF) of the substrates before and after coating with PAN and PAN/CuBTC nanofibers are presented in Table 3.

As shown in Table 3, the order of the substrates from highest to lowest filtration efficiency was as follows: MB25 > MB15 > S > TF > C > SB30 > SB25, indicating that the meltblown fabric with a grammage of 25 g/m^2 (MB25) had the highest filtration efficiency, while the spunbond fabric with a grammage of 25 g/m^2 (SB25) had the lowest efficiency. Additionally, the order of substrates in terms of pressure drop from lowest to highest was as follows: T, MB25, C, MB15, SB30, SB25, and S. Based on the obtained results, Tetron fabric (TF-F) with a base weight of 96.4 g/m^2 exhibited the highest resistance to air passage, whereas SSMMS fabric (S-F) with a base weight of 30.121 g/m^2 had the lowest pressure drop.

These results showed that although melt blownfabric, which is used in the most commercially RPEs as the main particle filtering layer, had a higher filtration efficiency than other fabrics, but the filtration efficiency of this fabric for 300 nm particles was less than 50 percent whilein Covid 19 Pandemic and many industrial and occupational environments, it is recommended to use N95 respirators [30,31], which have a minimum efficiency of 95 % for 300 nm particles therefore, in order to achieve higher efficiency, manufacturers use several layers of melt blown and spunbond fabrics in the structure of respirators, which greatly affects the breathability of them

Table 3
MFE-300nm, DP and QF of the substrates before and after coating with PAN and PAN/CuBTC nanofibers.

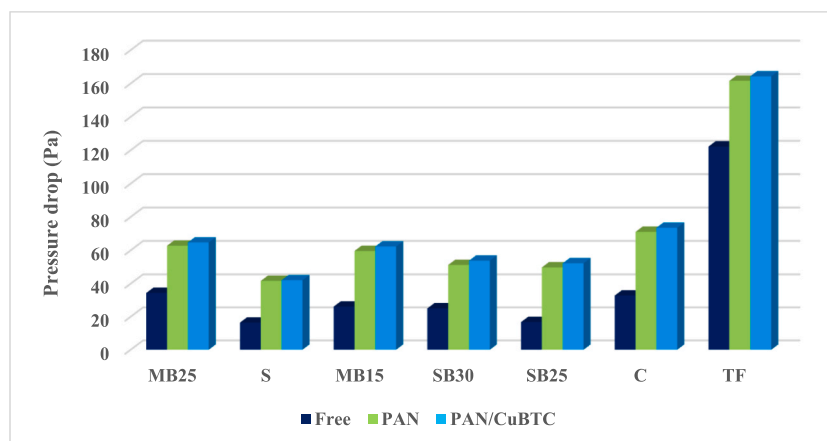| Sample Code	Nanofiber Coating	Base weight (g/m^2)	DP (Pa) ± SD	MFE-300nm ± SD	Quality factor (Pa^{-1})
SB25-F	–	24.843	16.78 ± 3.09	19.01 ± 1.10	0.012
SB25-P	PAN	0.141	49.82 ± 12.21	90.21 ± 0.63	0.046
SB25-PC	PAN/CuBTC	0.128	52.29 ± 6.19	95.14 ± 0.98	0.052
SB30-F	–	30.365	25.08 ± 4.83	19.35 ± 0.79	0.008
SB30-P	PAN	0.138	51.28 ± 7.15	93.44 ± 0.68	0.051
SB30-PC	PAN/CuBTC	0.131	53.84 ± 2.36	95.52 ± 1.16	0.055
MB15-F	–	14.875	26.14 ± 4.55	36.74 ± 1.01	0.017
MB15-P	PAN	0.143	59.67 ± 2.72	93.33 ± 0.81	0.048
MB15-PC	PAN/CuBTC	0.122	52.33 ± 6.17	98.02 ± 1.21	0.074
MB25-F	–	25.145	34.40 ± 3.46	41.22 ± 1.31	0.016
MB25-P	PAN	0.137	62.81 ± 2.17	96.41 ± 1.06	0.052
MB25-PC	PAN/CuBTC	0.126	64.77 ± 4.08	98.45 ± 1.19	0.064
S-F	–	30.121	16.46 ± 2.15	32.46 ± 1.11	0.023
S-P	PAN	0.140	41.71 ± 3.78	96.22 ± 0.81	0.072
S-PC	PAN/CuBTC	0.127	42.11 ± 2.44	98.31 ± 0.92	0.094
C-F	–	39.121	32.84 ± 5.44	23.40 ± 0.49	0.008
C-P	PAN	0.142	71.11 ± 1.24	93.11 ± 1.11	0.037
C-PC	PAN/CuBTC	0.121	73.56 ± 4.28	96.75 ± 0.85	0.046
TF-F	–	96.402	122.21 ± 15.78	27.43 ± 1.26	0.002
TF-P	PAN	0.144	161.61 ± 11.02	93.46 ± 1.22	0.016
TF-PC	PAN/CuBTC	0.129	164.32 ± 9.87	97.22 ± 0.96	0.021

[32,33].

The higher filtration efficiency of melt blown compared to other substrates could be related to the smaller fiber diameter. The role of reducing the diameter of fibers on improving the filtration efficiency of substrates has been emphasized in various studies, which is also in accordance with the filtration theory [34].On the other hand, spunbond substrates possess greater strength and lower pressure dropcompared to melt blown substrates [35,36]. The results of the present study indicated that composite substrates, such as SSMMS, which combine the characteristics of meltblown and spunbond substrates, have better quality factors compared to other substrates due to their structural integrity, filtration efficiency, and appropriate pressure drop. Therefore, they are a suitable option for use as supportive layer of nanofiber coatings.

The pressure drop across the substrate before and after coating with PAN and PAN/CuBTC nanofibers was plotted in Fig. 3.

As can be seen from Fig. 3, the highest pressure drop before coating nanofibers (122.21 ± 15.78 Pa) occurred over the Tetron fabric (TF-F) and the pressure drop of SB25 and SSMMS(S) were lower than others.

As illustrated in Fig. 3, the highest pressure drop before coating nanofibers (122.21 ± 15.78 Pa) was observed over the Tetron fabric (TF-F), while the pressure drops of SB25 and SSMMS (S) were lower than those of the others. Although various factors such as packing density, fiber diameter, and thickness affect the pressure drop of the fabrics, studies have indicated that due to structural differences, the pressure drop of woven fabrics is greater than that of non-woven fabrics [34].In this study, the Tetron fabric, the only woven substrate examined, exhibited a higher pressure drop compared to nonwoven substrates.

Previous researches have demonstrated that increasing thickness, packing density, and reducing fiber diameter not only enhance efficiency but also lead to an increase in the pressure drop of the substrates. Substrates with a high respiratory pressure drop may not be suitable for users [24,37–39]. Thus, a balance between these two parameters must be considered in the design and selection of RPEs for

Fig. 3. The pressure drop across the substrate before and after coating with PAN and PAN/CuBTC nanofibers.

various applications. To compare the performance of RPEs while considering both efficiency and respiratory pressure drop, the quality factor is employed, defined as the ratio of the filtration efficiency of particles with a diameter of 300 nm to the respiratory pressure drop of the respirators [6].

As shown in Table 2, the SSMMS substrates achieved the highest quality factor due to their low pressure drop and relatively high filtration efficiency compared to other fabrics, while the Tetron fabric had the lowest quality factor owing to its high pressure drop. The quality factor values of the other substrates were similar. The results indicated that the Tetron fabric, used during the COVID-19 pandemic, exhibited relatively low filtration efficiency despite the high respiratory pressure drop, suggesting that these fabrics are not recommended for use in respirator structures.

On the other hand, although the results indicated that the SSMMS substrate had a lower filtration efficiency compared to the MB25 and MB15 substrates (32.46 % vs. 41.22 % and 36.74 %, respectively), the quality factor of the SSMMS fabric was better due to its lower pressure drop (0.023 Pa-1 vs. 0.016 Pa-1 and 0.017 Pa-1, respectively).

3.2. Filtration performance of substrates after coating with PAN and PAN/CUBTC nanofibers

The results obtained clearly demonstrated that applying a single nanofiber layer of PAN or PAN/Cu-BTC on conventional substrates significantly enhanced their filtration efficiency. As illustrated in Fig. 4, the filtration efficiency of all substrates coated with PAN (Fig. 4-a) or PAN/Cu-BTC (Fig. 4-b) nanofibers in the particle size range of 300–1000 nm exceeded 90 % and 95 %, respectively.

As shown in Table No. 2, the order of PAN and PAN/CuBTC coated nanofibers from highest to lowest filtration efficiency in MPPS was as follows: MB25-P > S-P > TF-P > SB30-P > MB15-P > C-P > SB25-P and MB25-PC > S-PC > MB15-PC > TF-PC > C-PC > SB30P > SB25P. All substrates coated with the PAN/CuBTC nanofibers exhibited efficiencies above 95 %, with the lowest filtration efficiency corresponding to SB25-PC at 95.14 % and the highest efficiency associated with MB25-PC, which achieved an efficiency of 98.45 % at
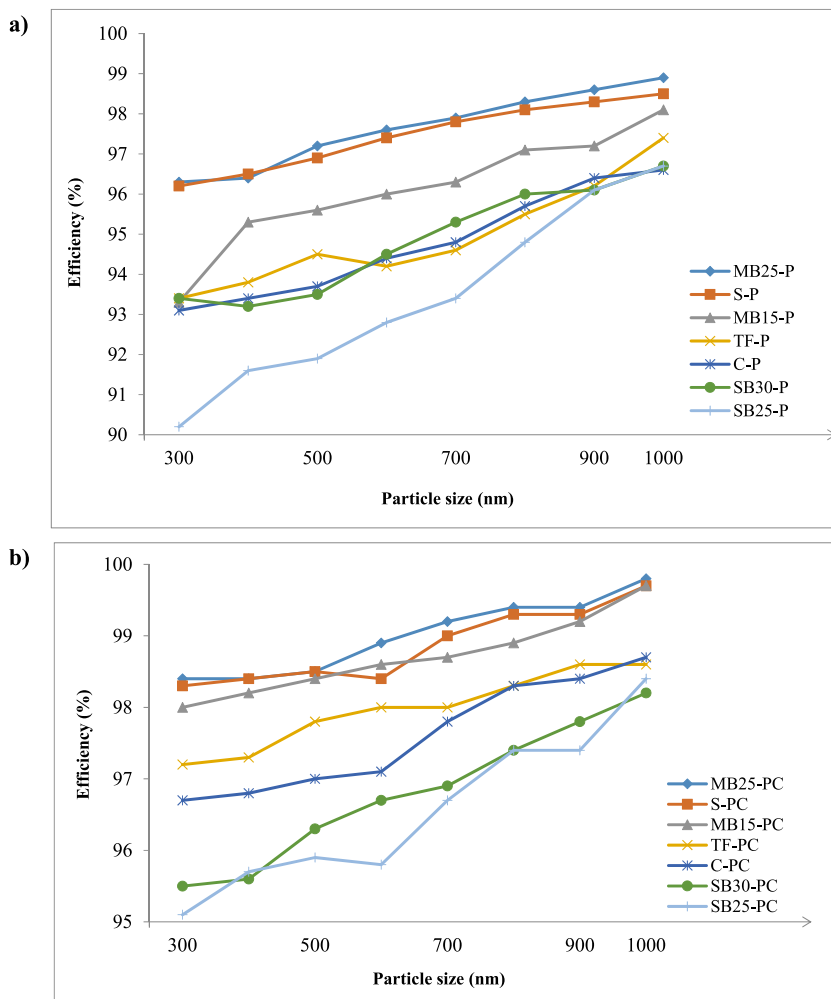

Fig. 4. The filtration efficiency of substrates coated with PAN (Fig. 4-a) or PAN/Cu-BTC (Fig. 4-b) nanofibers in the particle size range of 300–1000 nm.

300 nm.

Fig. 5 illustrates the reduction ratio of particle penetration (P_{before}-P_{after}) at 300 nm after coating the substrates with PAN and PAN/CuBTC nanofibers.

As shown in Fig. 5, the reduction ratio of penetration of 300 nm particles after coating the substrates with PAN nanofibers varies from a minimum of 8.27 times to a maximum of 17.87 times for different substrates. For substrates coated with PAN/CuBTC nanofibers, this ratio ranges between 16.66 and 39.96 times. For example, the coating of the SSMMS substrate with PAN and PAN/CuBTC nanofibers reduces the penetration of 300 nm particles by 17.87 and 39.96 times, respectively, compared to the uncoated state, which is a significant amount.

In a study, Sharabi et al. found that a polyamide 66 nanofiber coating on an SMS substrate for 60 min could increase the filtration efficiency of 300 nm particles from 35.03 % to approximately 98.66 %. This represents a 48-fold reduction in particle penetration, aligning with the results of the present study [40].

The results shown in Fig. 3 suggested that the addition of PAN and PAN/CuBTC nanofibers to the substrates increased their pressure drop compared to the pure state, with an average increase of about 30 and 35 Pa, respectively. The lowest pressure drop in the coated substrates was observed in the S-P and S-PC layers, which measured 41.71 ± 3.78 Pa and 42.11 ± 2.44 Pa, respectively, while the highest pressure drop of 161.61 ± 11.02 Pa and 165.32 ± 9.87 Pa was related to the TF-P and TF-PC layers, respectively. The pressure drop created by the PAN/CuBTC nanofibers was only slightly higher than that of the PAN nanofiber layer, except for MB15, where the pressure drop was greater for the PAN media (MB15-P = 59.67 Pa, MB15-PC = 52.33 Pa).

The effect of the nanofibers on the pressure drop of the substrates has been investigated by other researchers, most of whom concluded that the nanofiber coatings moderately lead to an increase in the pressure drop of the final media; on the other hand, the increase in filtration efficiency, especially in MPPS, has improved the quality factor of substrates coated with nanofibers [25,41].

Li et al. investigated the filtration performance of polyvinyl alcohol (PVA)/zeolite imidazole frameworks-8 (ZIF-8) with a polypropylene (PP) melt blown substrate and found that, compared to the very low filtration efficiency of the PP melt blown substrate, the efficiency of PP/PVA/ZIF-8 increased up to 100 %, depending on the amount of ZIF-8 added to the electrospinning solution [42].

The results indicated that the type of substrate used for coating with nanofibers significantly affects the quality factor of the resulting filtration media. As shown in Table 2, the order of the quality factor for substrates coated with nanofibers was as follows: S, MB25, MB15, SB30, SB25, C, and TF, respectively. The highest quality factor values before and after coating with PAN and PAN/CuBTC nanofibers corresponded to the SSMMS substrates, with values of 0.023, 0.072, and 0.094 Pa^{-1}, while the lowest quality factor values were associated with Tetron, which had values of 0.002, 0.016, and 0.021 Pa^{-1}, respectively. It should be noted that MB25-F ranked higher than S-F and MB15-F in terms of filtration efficiency, but its quality factor was lower due to a higher pressure drop. The other two materials, SB30 and SB25, in both non-coated and coated states with PAN and PAN/CuBTC nanofibers, ultimately exhibited a higher quality factor due to a lower pressure drop, despite having lower efficiency compared to Activated Carbon and Tetron substrates.

As shown in Table No. 2, the substrates coated with PAN/CuBTC generally exhibited a higher quality factor than those coated with PAN alone. This suggests that the combination of PAN nanofibers with CuBTC nanoparticles has enhanced the filtration properties of the substrates. This improvement may be attributed to the influence of adding CuBTC nanoparticles on the characteristics of the electrospinning polymeric solution, ultimately altering the structure of the nanofibers. As indicated in Table 1, the mean diameter of PAN/CuBTC nanofibers was smaller compared to that of pure PAN nanofibers (227 nm vs. 332 nm).

In general, the results of the present study indicate that fiber diameter is one of the most important parameters affecting the filtration performance of substrates. Among the substrates examined, the filtration efficiency of melt blown and SSMMS composite substrates was superior due to the use of fibers with smaller diameters. Additionally, coating these substrates with nanofibers, which have significantly smaller diameters, enhances the filtration mechanisms for fine particles such as direct interception, diffusion, and electrostatic precipitation resulting from surface charge, thereby improving the filtration performance of the substrates used in RPEs. Furthermore, the combined use of nanofibers and microfiber substrates mitigates the limitations of nanofiber coatings, such as low mechanical strength and the potential for nanofiberrelease from the substrates, enabling the use of these substrates in composite and multilayer structures. Another limitation of using nanofiber substrates in RPEs is the significant increase in pressure drop with
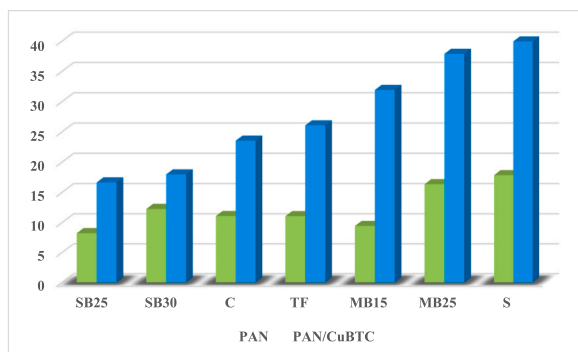

Fig. 5. The reduction ratio of penetration of 300 nm particles after covering the substrates with PAN and PAN/CuBTC nanofibers.

increasing thickness, which can be effectively addressed by the layered use of nanofibrous and microfiber substrates, as supported by various studies [43–45]. Therefore, the combined use of microfiber and nanofiber substrates can enhance the filtration performance by increasing the thickness of the substrates and the particle loading capacity.

Additionally, the enhancement of surface charge retention and improvement of deposition mechanisms due to electrostatic forces, leading to increased filtration efficiency in nanofibers functionalized with metallic nanoparticles, has also been confirmed in other studies [14,46].

The results of this study indicated that while the combination of nanofiber coatings enhances the filtration properties of all microfiber substrates, microfibers with a lower pressure drop, such as SSMMS fabric, can yield a higher quality factor when combined with nanofibers.

4. Conclusions

In this study, seven types of common substrates used in respiratory protective masks were coated with PAN and PAN/CuBTC nanofibers, and their filtration performance was evaluated. The results indicated that nanofiber coatings, due to their unique properties such as small fiber diameter, can enhance the filtration characteristics of all types of microfiber substrates, particularly in MPPS. The limiting factor in the combined use of microfiber and nanofiber is the initial pressure drop of the microfiber.

The main findings of this study can be summarized as follows:

1) The integration of nanofibers with conventional substrates used in the construction of personal protective equipment not only addresses the limitations associated with the use of nanofibers in RPEs, such as low mechanical strength and the inability to increase thickness due to increased pressure drop, but also leads to a significant improvement in filtration efficiency and the quality factor of composite substrates.
2) Nanofiber coatings can be used to improve the filtration performance of all common substrates used in RPEs.
3) The type and properties of microfiber substrates has an effect on the quality factor of the final composite filtering media, and the results of the study showed that the SSMMS substrate due to its lower pressure drop had highest value of quality factor after coating with nanofibers.
4) Incorporation of nanoparticles such as metal and organic frameworks with nanofibers can lead to the improvement of the quality of the final filtration Media. Also, these nanoparticles can create multi-functional capabilities in the final filtration media due to properties such as surface absorption of gaseous pollutants and antimicrobial properties.

CRediT authorship contribution statement

Majid Habibi Mohraz: Writing – review & editing, Writing – original draft, Supervision, Formal analysis, Data curation, Conceptualization. **Adel Jafari:** Methodology, Investigation. **Mobina Khezrian:** Methodology, Data curation.

Data availability statement

Research related Data is not stored in publicly available repositories, and Data will be made available on request.

Ethics declarations

Ethical approval for this study was obtained from Research ethical committee of Hamadan university of medical sciences (IR. UMSHA.REC.1403.697).

Declaration of competing interest

The authors declare that they have no known competing financial interests or personal relationships that could have appeared to influence the work reported in this paper.

References

[1] K. O'Dowd, et al., Face masks and respirators in the fight against the COVID-19 pandemic: a review of current materials, advances and future perspectives, Materials 13 (15) (2020) 3363.

[2] P.T. O'Shaughnessy, et al., Validation of N95 respirator models for pressure drop and particle capture efficiency, J. Occup. Environ. Hyg. 20 (9) (2023) 390–400.

[3] C. Brochot, M.N. Saidi, A. Bahloul, How effective is the filtration of 'KN95' filtering facepiece respirators during the COVID-19 pandemic? Annals of work exposures and health 65 (3) (2021) 358–366.

[4] W. Hao, et al., Filtration performances of non-medical materials as candidates for manufacturing facemasks and respirators, Int. J. Hyg Environ. Health 229 (2020) 113582.

[5] M. Liao, et al., A technical review of face mask wearing in preventing respiratory COVID-19 transmission, Curr. Opin. Colloid Interface Sci. 52 (2021) 101417.

[6] F.G. Morais, et al., Filtration efficiency of a large set of COVID-19 face masks commonly used in Brazil, Aerosol. Sci. Technol. 55 (9) (2021) 1028–1041.

[7] S. Duncan, P. Bodurtha, S. Naqvi, The protective performance of reusable cloth face masks, disposable procedure masks, KN95 masks and N95 respirators: filtration and total inward leakage, PLoS One 16 (10) (2021) e0258191.

[8] L.H. Kwong, et al., Review of the breathability and filtration efficiency of common household materials for face masks, ACS Nano 15 (4) (2021) 5904–5924.

[9] R. Al-Attabi, et al., Durable and comfortable electrospun nanofiber membranes for face mask applications, Sepur. Purif. Technol. 322 (2023) 124370.

[10] W.A. Abbas, et al., Cost-effective face mask filter based on hybrid composite nanofibrous layers with high filtration efficiency, Langmuir 37 (24) (2021) 7492–7502.

[11] C. Akduman, E. Akcakoca Kumbasar, Nanofibers in face masks and respirators to provide better protection, in: IOP Conference Series: Materials Science and Engineering, IOP Publishing, 2018.

[12] M. Chen, et al., Graphene oxide functionalized polyvinylidene fluoride nanofibrous membranes for efficient particulate matter removal, J. Membr. Sci. 635 (2021) 119463.

[13] F.S. Victor, et al., Electrospun nanofibers of polyvinylidene fluoride incorporated with titanium nanotubes for purifying air with bacterial contamination, Environ. Sci. Pollut. Control Ser. 28 (2021) 37520–37533.

[14] M. Hu, et al., Zeolitic-imidazolate-framework filled hierarchical porous nanofiber membrane for air cleaning, J. Membr. Sci. 594 (2020) 117467.

[15] Y. Lou, et al., A versatile electrospun polylactic acid nanofiber membrane integrated with halloysite nanotubes for indoor air purification, disinfection, and photocatalytic degradation of pollutants, Sepur. Purif. Technol. 323 (2023) 124371.

[16] Y. Bian, et al., Effective removal of particles down to 15 nm using scalable metal-organic framework-based nanofiber filters, Appl. Mater. Today 20 (2020) 100653.

[17] K. Lee, D. Kim, J. Kim, Computational modeling of multiscale air filter media consisting of nano-and microfibers, ACS Appl. Nano Mater. 6 (11) (2023) 9415–9425.

[18] V.V. Kadam, L. Wang, R. Padhye, Electrospun nanofibre materials to filter air pollutants–A review, J. Ind. Textil. 47 (8) (2018) 2253–2280.

[19] H.T. Le, et al., Efficient and recyclable Cu 2 (BDC) 2 (BPY)-catalyzed oxidative amidation of terminal alkynes: role of bipyridine ligand, Catal. Sci. Technol. 5 (2) (2015) 851–859.

[20] S. Chattopadhyay, T.A. Hatton, G.C. Rutledge, Aerosol filtration using electrospun cellulose acetate fibers, J. Mater. Sci. 51 (2016) 204–217.

[21] S. Alizadeh, D. Nematollahi, Convergent and divergent paired electrodeposition of metal-organic framework thin films, Sci. Rep. 9 (1) (2019) 14325.

[22] N. Sani, W. Lau, A. Ismail, Polyphenylsulfone-based solvent resistant nanofiltration (SRNF) membrane incorporated with copper-1, 3, 5-benzenetricarboxylate (Cu-BTC) nanoparticles for methanol separation, RSC Adv. 5 (17) (2015) 13000–13010.

[23] P. Khude, Nanofibers for high efficiency filtration, J. Mater. Sci. Eng. 6 (6) (2017) 1–10.

[24] Y. Bian, et al., Influence of fiber diameter, filter thickness, and packing density on PM2. 5 removal efficiency of electrospun nanofiber air filters for indoor applications, Build. Environ. 170 (2020) 106628.

[25] Y. Zhou, et al., Electrospun nanofiber membranes for air filtration: a review, Nanomaterials 12 (7) (2022) 1077.

[26] Y. Liu, et al., Preparing micro/nano-fibrous filters for effective PM 2.5 under low filtration resistance, Chem. Eng. Sci. 217 (2020) 115523.

[27] L.M. Valencia-Osorio, M.L. Álvarez-Láinez, Global view and trends in electrospun nanofiber membranes for particulate matter filtration: a review, Macromol. Mater. Eng. 306 (10) (2021) 2100278.

[28] Z. Xiong, et al., An ultralow base weight of nanocellulose boosting filtration performance of hierarchical composite air filter inspired by native spider web, Compos. B Eng. 226 (2021) 109342.

[29] M. Pardo-Figuerez, et al., Antimicrobial nanofiber based filters for high filtration efficiency respirators, Nanomaterials 11 (4) (2021) 900.

[30] J.J. Bartoszko, et al., Medical masks vs N95 respirators for preventing COVID-19 in healthcare workers: a systematic review and meta-analysis of randomized trials, Influenza and other respiratory viruses 14 (4) (2020) 365–373.

[31] M. Zhang, et al., Masks or N95 respirators during COVID-19 pandemic–which one should I wear? J. Oral Maxillofac. Surg. 78 (12) (2020) 2114–2127.

[32] Silva, C., et al., Behaviour Assessment of Tridimensional Multilayer Fibrous Structures as Respiratory Protection Substrates.

[33] J. Fontenot, Filtration Efficiency and Breathability of Fabric Masks and Their Dependence on Fabric Characteristics, Colorado State University, 2022.

[34] H.B. Kim, et al., Filter quality factors of fibrous filters with different fiber diameter, Aerosol. Sci. Technol. 55 (2) (2021) 154–166.

[35] D. Radchuk, et al., The study of the mechanical strength of polypropylene filter material for the production of disposable respirators, Solid State Phenom. 364 (2024) 89–100.

[36] E. Shim, et al., Improvement of polytetrafluoroethylene membrane high-efficiency particulate air filter performance with melt-blown media, Polymers 13 (23) (2021) 4067.

[37] W.W.-F. Leung, C.-H. Hung, P.-T. Yuen, Effect of face velocity, nanofiber packing density and thickness on filtration performance of filters with nanofibers coated on a substrate, Sepur. Purif. Technol. 71 (1) (2010) 30–37.

[38] S.-H. Hung, et al., Optimizing the packing density and chemistry of cellulose nanofilters for high-efficiency particulate removal, Ind. Eng. Chem. Res. 60 (43) (2021) 15720–15729.

[39] M. Monjezi, H. Jamaati, The effects of face mask specifications on work of breathing and particle filtration efficiency, Med. Eng. Phys. 98 (2021) 36–43.

[40] S. Shahrabi, A.A. Gharehaghaji, M. Latifi, Fabrication of electrospun polyamide-66 nanofiber layer for high-performance nanofiltration in clean room applications, J. Ind. Textil. 45 (5) (2016) 1100–1114.

[41] S. Ullah, et al., Reusability comparison of melt-blown vs nanofiber face mask filters for use in the coronavirus pandemic, ACS Appl. Nano Mater. 3 (7) (2020) 7231–7241.

[42] T.-T. Li, et al., Polypropylene/polyvinyl alcohol/metal-organic framework-based melt-blown electrospun composite membranes for highly efficient filtration of PM2. 5, Nanomaterials 10 (10) (2020) 2025.

[43] W. Ma, et al., Multi-layered micro/nano filters for efficient air filtration, in: Civil Engineering and Energy-Environment, vol. 1, CRC Press, 2023, pp. 446–452.

[44] L. Kang, et al., Preparation of electrospun nanofiber membrane for air filtration and process optimization based on BP neural network, Mater. Res. Express 8 (11) (2021) 115010.

[45] Y. Xu, et al., Multi-layered micro/nanofibrous nonwovens for functional face mask filter, Nano Res. 15 (8) (2022) 7549–7558.

[46] J. Guo, et al., PAA@ ZIF-8 incorporated nanofibrous membrane for high-efficiency PM2. 5 capture, Chem. Eng. J. 405 (2021) 126584.